

# Analytical Methods

Accepted Manuscript



This is an *Accepted Manuscript*, which has been through the Royal Society of Chemistry peer review process and has been accepted for publication.

*Accepted Manuscripts* are published online shortly after acceptance, before technical editing, formatting and proof reading. Using this free service, authors can make their results available to the community, in citable form, before we publish the edited article. We will replace this *Accepted Manuscript* with the edited and formatted *Advance Article* as soon as it is available.

You can find more information about *Accepted Manuscripts* in the [Information for Authors](#).

Please note that technical editing may introduce minor changes to the text and/or graphics, which may alter content. The journal's standard [Terms & Conditions](#) and the [Ethical guidelines](#) still apply. In no event shall the Royal Society of Chemistry be held responsible for any errors or omissions in this *Accepted Manuscript* or any consequences arising from the use of any information it contains.

Cite this: DOI: 10.1039/c0xx00000x

www.rsc.org/xxxxxx

COMMUNICATION

# A new label-free and turn-on fluorescence probe for hydrogen peroxide and glucose detection based on DNA–silver nanoclusters

Hui-Xia Han, Xue Tian, Xiang-Juan Kong, Ru-Qin Yu and Xia Chu\*

Received (in XXX, XXX) Xth XXXXXXXXXX 20XX, Accepted Xth XXXXXXXXXX 20XX

DOI: 10.1039/b000000x

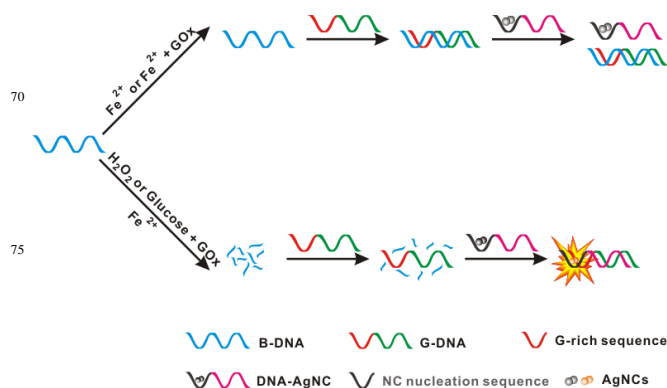
We have developed a reliable, sensitive, label-free and turn-on sensor for H<sub>2</sub>O<sub>2</sub> and glucose based on the cleavage of ssDNA by •OH and the fluorescence enhancement effect when guanine-rich (G-rich) DNA sequences are in proximity to DNA-silver nanoclusters (DNA-Ag NCs). In addition, we also prove that •OH is indeed produced in the sensing by adding antioxidants.

H<sub>2</sub>O<sub>2</sub> is one of the most important reactive oxygen species, it is involved in many biological, chemical, pharmaceutical, clinical, food and environmental processes. However, the wide use of H<sub>2</sub>O<sub>2</sub> in various fields has resulted in serious health and environmental problems. Since H<sub>2</sub>O<sub>2</sub> may cause various human central nervous system diseases<sup>1-2</sup> and has an indirect effect on the procedure of acid rain,<sup>3</sup> which currently is a global problem. Therefore, the detection of H<sub>2</sub>O<sub>2</sub> is of great importance. Traditional techniques, such as titrimetry,<sup>4</sup> spectrophotometry,<sup>5-6</sup> electroanalysis,<sup>7-8</sup> resonance light scattering assays,<sup>9-10</sup> chromatography<sup>11-12</sup> and so on, have been applied to the determination of H<sub>2</sub>O<sub>2</sub>. However, these conventional methods suffer from expensive, time-consuming, laborious, isotope labeling, high background, low signal-to-noise ratio (S/N ratio), less sensitive<sup>5,13</sup> and poor selectivity<sup>14</sup> which restrict their widespread use.

Glucose is one of the major carbohydrate metabolized by animals and plants, it is the main source of energy in cellular metabolism and plays an important role in the natural growth of cells. It is also important in the food industry,<sup>15</sup> public health,<sup>16</sup> the life sciences,<sup>17</sup> and other industry sectors. The glucose level in urine or blood<sup>18</sup> is usually acted as a clinical indicator of diabetes. Therefore, developing sensitive and novel methods for detecting glucose is very important. Common protocols performed for detecting glucose are surface plasmon resonance,<sup>19</sup> electrochemiluminescence,<sup>20</sup> colorimetry,<sup>21</sup> optical,<sup>22-23</sup> and electrochemical.<sup>24-25</sup> However, many existing techniques for detection of glucose suffer from isotope labeling, high background, low signal-to-noise ratio

(S/N ratio), less sensitive and have poor specificity for biological fluids.<sup>26</sup> At the present time, the determination of glucose is generally based on H<sub>2</sub>O<sub>2</sub> measurement, as glucose can be oxidized by O<sub>2</sub> producing hydrogen peroxide (H<sub>2</sub>O<sub>2</sub>) in the presence of glucose oxidase (GOx).<sup>27-30</sup> Thus, the accurate determination of glucose is dependent on the accurate determination of H<sub>2</sub>O<sub>2</sub>.

Noble metals nanoclusters, comprising of several to several tens of atoms, such as gold, silver and Pt nanoclusters, have obtained much attention owing to their particular fluorescence properties and have great potential for applications in biosensors and bionanotechnology.<sup>31-32</sup> Among these noble metal clusters, silver nanoclusters, which possess good water solubility, desirable photophysical properties and low toxicity,<sup>33</sup> complements the properties of organic dyes and quantum dots.<sup>34-35</sup> Among various templates of Ag nanoclusters, oligonucleotide-templated silver nanoclusters (DNA–Ag NCs) have become of great interest due to their facile synthesis, strong and robust size, tunable fluorescence emission, and high photostability.<sup>36-37</sup> The fluorescence emission spectra of DNA–Ag NCs can be tuned throughout the visible and near infrared range region by changing oligonucleotides, which are the template of silver nanoclusters.<sup>38</sup> Numerous schemes that related to silver nanoclusters have been designed based on the quenching



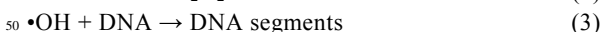
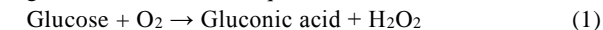
**Scheme 1** Schematic description of the label-free and turn-on strategy for H<sub>2</sub>O<sub>2</sub> and glucose detection based on the cleavage of ssDNA by •OH and the fluorescence enhancement effect when guanine-rich (G-rich) DNA sequences are in proximity to DNA-silver nanoclusters (DNA-Ag NCs).

State Key Laboratory of Chemo/Bio-Sensing and Chemometrics, College of Chemistry and Chemical Engineering, Hunan University, Changsha, 410082, P. R. China. E-mail: xiachu@hnu.edu.cn; Fax: +86-731-88821916; Tel: +86-731-88821916

† Electronic Supplementary Information (ESI) available: Experimental details and supplementary figures. See DOI: 10.1039/b000000x

mechanism. As a large amount of ligands or solvents may interfere with quenching and lead to “false positive”, they are not preferred in practice.<sup>39</sup> Lately, Werner and colleagues discovered an interesting phenomenon that the fluorescence intensity of DNA–Ag NCs could be enhanced when guanine-rich (G-rich) DNA sequences were in close proximity to them. It has been proposed to be an advanced approach to develop “turn-on” nanoclusters biosensors.<sup>40–42</sup> More “turn on” homogeneous assays would be desirable for a broader class of targets.

Herein, Inspired by the above facts, we developed a reliable, sensitive, label-free and turn-on sensor for H<sub>2</sub>O<sub>2</sub> and glucose based on the cleavage of ssDNA by •OH<sup>28,30</sup> and the fluorescence enhancement effect when guanine-rich (G-rich) DNA sequences are in proximity to DNA-silver nanoclusters (DNA-Ag NCs). The mechanism of the label-free and turn-on fluorescent assay of H<sub>2</sub>O<sub>2</sub> and glucose are illustrated with Scheme 1. The system mainly consists of block DNA (B-DNA), G-DNA and Ag-DNA. B-DNA, which can be entirely complementary to G-DNA, plays the role as the substrate of •OH. Except being entirely complementary to B-DNA, G-DNA, which contains a guanine-rich overhang sequence (red part in Scheme 1) and a hybridization part (green part in Scheme 1) at the 5'-end, is partially complementary to Ag-DNA. Ag-DNA involves two sequences, one sequence (rose red part in Scheme 1) is complementary to G-DNA and the other sequence (black part in Scheme 1) is used to compound DNA-Ag NCs. The DNA-Ag NCs through the reduction of Ag ions by NaBH<sub>4</sub> display a dark fluorescence emission. The fluorescence enhancement obviously when G-rich DNA sequences are in proximity to DNA-Ag NCs. In the absence of H<sub>2</sub>O<sub>2</sub>, B-DNA hybridized with G-DNA, DNA-Ag NCs, which failed to hybridize with G-DNA, displayed very weak fluorescence. When H<sub>2</sub>O<sub>2</sub> was introduced into the system, the hydroxyl radical (•OH) was produced by Fenton reaction in the presence of ferrous iron (Fe<sup>2+</sup>). As the oxidative effect of •OH, B-DNA was irreversibly cleaved into mono- or short-oligonucleotides fragment through hydrogen abstraction from the deoxyribose phosphate backbones<sup>43</sup>, so it could not hybridize with G-DNA. Thus, G-DNA hybridized with Ag-DNA, the G-rich sequences were brought in proximity to Ag NCs, accompanied by a significant fluorescence enhancement. Therefore, H<sub>2</sub>O<sub>2</sub> was successfully quantified by monitoring the fluorescence intensity. Because glucose can be oxidized by O<sub>2</sub> producing hydrogen peroxide (H<sub>2</sub>O<sub>2</sub>) in the presence of glucose oxidase (GOx),<sup>27–29</sup> so this system can also quantify glucose. The reaction equations are as follows:



(In these reactions, EDTA prevents iron ions from binding to DNA and accelerates the formation of hydroxyl radical.<sup>43</sup>) Besides, we also proved that •OH was indeed produced in the sensing system by adding antioxidants. This label-free and turn-on biosensor have turned out to be sensitive and selective.

Gel electrophoresis analysis was used to demonstrate the breakage of B-DNA. As shown in Fig. 1, the B-DNA alone (lane 2) showed a clear band between 20 bases and 30 bases.

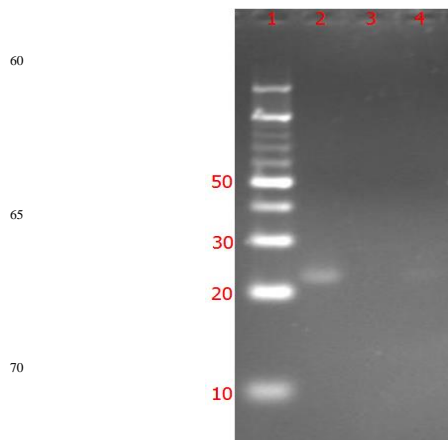


**Fig.1** Gel electrophoresis analysis of B-DNA strand scission. DNA ladder (lane 1), 1 μM B-DNA alone (lane 2), 1 μM B-DNA incubated with H<sub>2</sub>O<sub>2</sub> and Fe<sup>2+</sup> (3 mM, 0.3 mM, respectively) (lane 3), 2 μM B-DNA incubated with glucose, GOx, and Fe<sup>2+</sup> (3.75 mM, 15 μg/ml, and 37.5 mM, respectively) (lane 4). The numbers in the left indicate the the number of the base.

When 1 μM B-DNA incubated with H<sub>2</sub>O<sub>2</sub> and Fe<sup>2+</sup> (lane 3), it could be observed that the DNA band disappeared, suggesting the breakage of the B-DNA chains by •OH completely. When 2 μM B-DNA incubated with glucose, GOx, and Fe<sup>2+</sup> (lane 4), we could see that the band almost completely disappeared, it suggested that almost all B-DNA chains were broken by •OH. The electrophoresis results have well confirmed the occurrence of Fenton reaction, which may lay the foundation for the further detection.

As shown in Fig. 2, Before hybridizing with G-DNA, DNA–Ag NCs showed very weak fluorescence emission at 510 nm with excitation at 465 nm (curves a and b, Fig. 2A). When G-DNA was introduced, the fluorescence intensity of Ag–DNA increased enormously, we also found that the excitation and emission peaks changed to 570 nm and 625 nm (curves c and d, Fig. 2A).

We first investigated the feasibility of our strategy for H<sub>2</sub>O<sub>2</sub> assay. Upon being excited at 570 nm, DNA–Ag NCs solely displayed very weak fluorescence (curve a, Fig. 2B). Upon the addition of G-DNA, the fluorescence intensity of the DNA–Ag NCs increased greatly in PB buffer (curve f, Fig. 2B), we also found that the fluorescence intensity increased more obviously in the sensing system after G-DNA was added (curve e, Fig. 2B), which may be caused by the solution environment of the sensing system. When the B-DNA was added into the system, B-DNA hybridized with G-DNA, the subsequent addition of DNA-Ag NCs could not hybridized with G-DNA, thus the fluorescence intensity of DNA-Ag NCs was not change (curve b, Fig. 2B). This result indicated that B-DNA could effectively prevent the fluorescence enhancement, which was caused by the proximity of G-rich sequences and the Ag NCs. When Fe<sup>2+</sup> and H<sub>2</sub>O<sub>2</sub> existed together in the sensing system, the fluorescence intensity increased obviously with a high signal-to-noise ratio (S/N ratio) about 123 (curve g, Fig. 2B). However, in the absence of H<sub>2</sub>O<sub>2</sub> or Fe<sup>2+</sup>, the fluorescence intensity was not

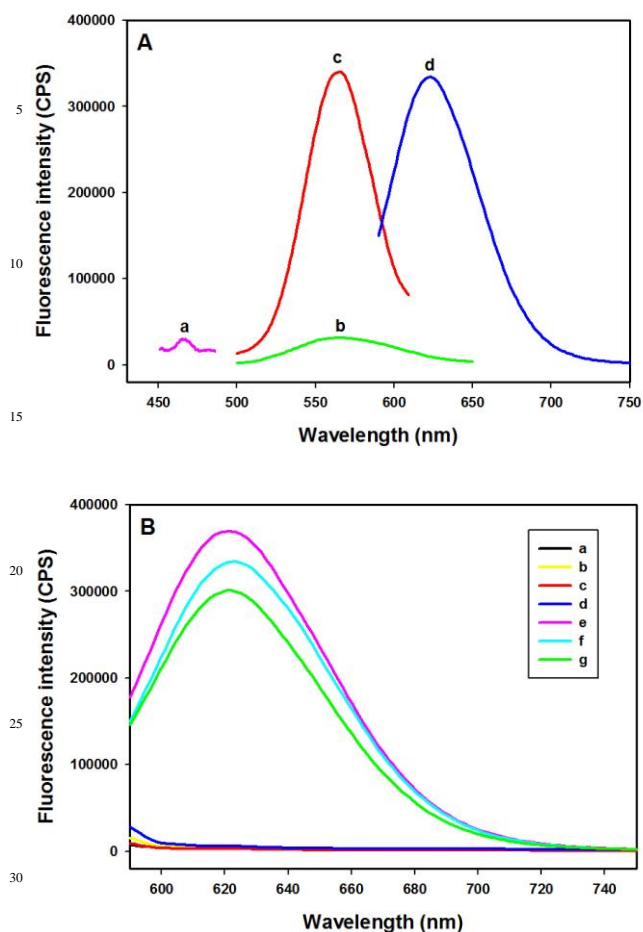


**Fig. 2** (A) Excitation and emission spectra of the fluorescent Ag NCs obtained before (curves a and b) and after (curves c and d) addition of G-DNA. The concentration of all DNA used here was 0.5  $\mu\text{M}$ . (B) The fluorescence emission spectra of DNA-Ag NCs were recorded in the presence of (a) no added reagent, (b) B-DNA + G-DNA, (c)  $\text{Fe}^{2+}$  + B-DNA + G-DNA, (d)  $\text{H}_2\text{O}_2$  + B-DNA + G-DNA, (e)  $\text{H}_2\text{O}_2$  +  $\text{Fe}^{2+}$  + G-DNA, (f) G-DNA, (g)  $\text{H}_2\text{O}_2$  +  $\text{Fe}^{2+}$  + B-DNA + G-DNA. The concentration of all DNA used here was 0.5  $\mu\text{M}$ . The concentration of  $\text{H}_2\text{O}_2$  was 3 mM.

enhancement (curve c and d, Fig. 2B). The result indicated that Fenton reaction produced  $\cdot\text{OH}$ , which cleaved B-DNA into mono- or short-oligonucleotides fragments. As a result, B-DNA could not hybridize with G-DNA and G-DNA formed a stable duplex with Ag-DNA, which brought G-rich sequences close to Ag NCs, accompanied by a significant fluorescence enhancement.

On the basis of the above work, the DNA-Ag NCs probe sensing system was used for detecting  $\text{H}_2\text{O}_2$ . Fig. 3A shows the fluorescent spectra of the sensing system in the presence of variable concentrations of  $\text{H}_2\text{O}_2$  (from 0 to 3 mmol/L). In the absence of  $\text{H}_2\text{O}_2$ , The fluorescence intensity of the system was very weak. However, the fluorescence intensity around 625 nm gradually enhanced upon increasing  $\text{H}_2\text{O}_2$  addition, this indicated that the B-DNA was gradually degradation. At high concentrations, however, the fluorescence increased

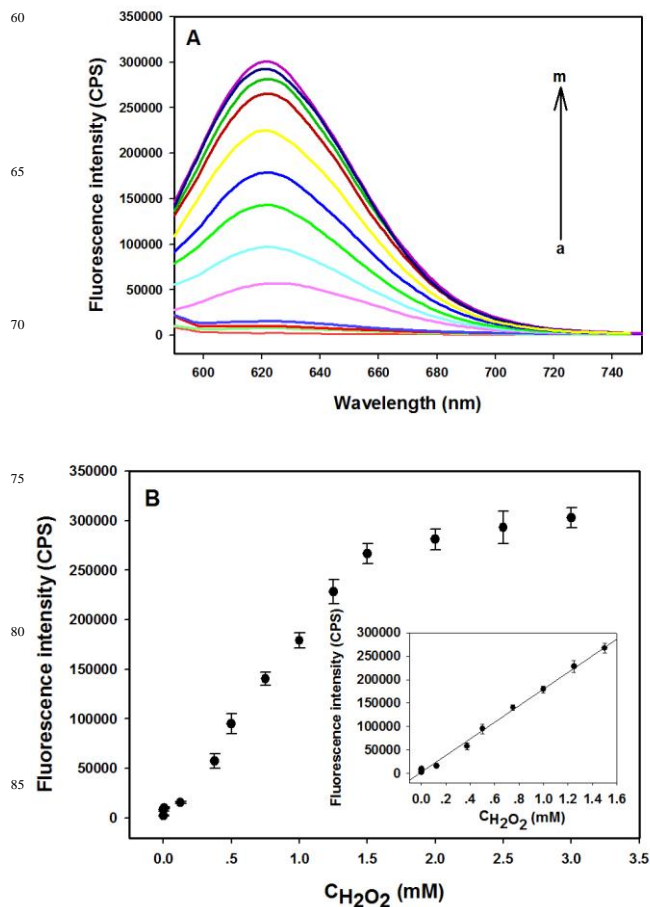


**Fig.3** (A) The fluorescence emission spectra of the sensing system with different concentrations of  $\text{H}_2\text{O}_2$  (from a to m): 0  $\mu\text{M}$ , 0.5  $\mu\text{M}$ , 5  $\mu\text{M}$ , 125  $\mu\text{M}$ , 375  $\mu\text{M}$ , 0.5 mM, 0.75 mM, 1 mM, 1.25 mM, 1.5 mM, 2 mM, 2.5 mM, 3 mM. (B) The relationship between the fluorescence intensity and the concentration of  $\text{H}_2\text{O}_2$ . Inset shows the linear relationship between the fluorescence increase and the concentration of  $\text{H}_2\text{O}_2$ . The concentration of DNA used here was all 0.5  $\mu\text{M}$ . Error bars represented standard deviations from three repeated experiments.

slowly in close to platform. This phenomenon is in agreement with the kinetics of enzyme-catalyzed reactions.<sup>44</sup> The relationship between the fluorescence intensity and the concentration of  $\text{H}_2\text{O}_2$  is outlined in Fig. 3B. As shown in the inset, a good linearity concentration ( $R^2 = 0.9960$ ) is raised from 0 to 1.5 mM. The detection limit (LOD) was 0.3  $\mu\text{M}$ , which is lower than those obtained using other reported fluorescence detection methods.<sup>45-46</sup> LOD was estimated based on the following equation:  $\text{LOD} = 3\sigma/k$  ( $\sigma$  is the standard deviation of the blank signals and  $k$  is the slope of the calibration curve).

The successful sensitive detection of  $\text{H}_2\text{O}_2$  was then applied for the analysis of glucose. We also first investigated the feasibility of our strategy for glucose assay. When  $\text{Fe}^{2+}$ , GOx and glucose existed together in the sensing system, the fluorescence intensity increased obviously with a high S/N ratio about 137 (Fig. S2h†). But the fluorescence intensity was much lower than that absence of B-DNA (Fig.S2f†). This

may be result from the incomplete breakage of B-DNA, which was proved by the gel electrophoresis analysis. However, in the absence of  $\text{Fe}^{2+}$ , GOx or glucose the fluorescence intensity was not enhancement (Fig.S2c-e†). This phenomenon was similar to  $\text{H}_2\text{O}_2$  detection (Fig.S1†, Fig.S2†).

To determine the optimum experimental conditions for glucose detection, we investigated the concentration of  $\text{Fe}^{2+}$  which is a moiety of the Fenton reagent, the concentration of GOx, the reaction time for B-DNA strand scission, and the incubation time for G-DNA hybridizing with DNA-Ag NCs in the sensing system. As shown in Fig. S3†, the fluorescence intensity ratio  $F/F_0$  increased rapidly as the concentration of  $\text{Fe}^{2+}$  was increased from 10 to 25  $\mu\text{M}$ , then changed slightly as the concentration of  $\text{Fe}^{2+}$  was further increased to 50  $\mu\text{M}$ . To ensure the amount of  $\text{Fe}^{2+}$  was enough, 37.5  $\mu\text{M}$  was chosen as the optimum concentration. Fig. S4† displays fluorescence enhancement of the sensing system at different concentrations of GOx, we can see that the fluorescence intensity increased

along with increasing GOx concentration over the range from 0 to 15  $\mu\text{g}/\text{mL}$  in the presence of glucose, and then reached a plateau, so 15  $\mu\text{g}/\text{mL}$  was the optimum concentration. As shown in Fig. S5†, the fluorescence intensity of the sensing system increased with the increase of reaction time for B-DNA strand scission from 0 to 6.5 h, suggesting the continuous cleavage of B-DNA. The fluorescence intensity increased slightly for reaction time greater than 4.5 h, indicating the cleavage of DNA was nearly finished in 4.5 h. Thus 4.5 h was chosen as the optimum reaction time. Fig. S6† shows the fluorescence enhancement of the sensing system at different incubation time for DNA-Ag NCs hybridizing with G-DNA. The fluorescence was measured every 10 min, the fluorescence enhancement was fast between 0 to 90 min and very slow after 90 min, it indicated that DNA-Ag NCs almost completely hybridized with G-DNA in 90 min. Therefore, 90 min was chosen as the optimum incubation time for DNA-Ag NCs hybridizing with G-DNA.

Under optimized condition, Fig. 4A shows the fluorescence emission spectra of the sensing system at varying concentrations of glucose. A very weak emission peak was observed before glucose addition. However, upon addition of glucose to the solution, the fluorescence intensity around 625 nm gradually enhanced upon the increasing of glucose concentration, and then changed slightly. This phenomenon is in agreement with the kinetics of enzyme-catalyzed reactions.<sup>44</sup> A good linearity concentration ( $R^2 = 0.9961$ ) was achieved by plotting the fluorescence increment versus glucose concentration within 0 to 3.75 mM, deriving a detection limit of 0.4  $\mu\text{M}$ , which is much lower than those obtained using other reported fluorescence detection methods.<sup>29,46-47</sup> LOD was calculated with the following equation:  $\text{LOD} = 3\sigma/k$  ( $\sigma$  is the standard deviation of the blank signals and  $k$  is the slope of the calibration curve) (Fig. 4B).

**Table 1** Determination of glucose in urine samples spiked with glucose.

| sample | added(mM) | found(mM) | recovery(%) | RSD(%) |
|--------|-----------|-----------|-------------|--------|
| 1      | 2.500     | 2.538     | 101.52      | 3.04   |
| 2      | 5.000     | 4.883     | 97.66       | 2.50   |
| 3      | 7.500     | 7.262     | 96.83       | 4.29   |

To evaluate the feasibility of the sensing system for glucose detection in biological samples, the proposed method was applied to detect glucose levels in urine samples spiked with glucose, as the presence of glucose in urine is an indication of worsening of diabetes. It is worth mentioning that Ag NCs can be quenched by  $-\text{SH}$ , so NEM which can eliminate  $-\text{SH}$  was firstly added to the samples incubating for 2 days to eliminate  $-\text{SH}$  which may be exist in urine samples. The results were shown in Table 1. We added different concentration of glucose to the three urine samples, the recoveries ranged from 96.83 % to 101.52 % for the three samples, and the relative standard deviation (RSD) were no more than 4.29 %. These results indicated that the proposed method can be used to detect glucose in urine.

Specificity was an important factor in evaluating the

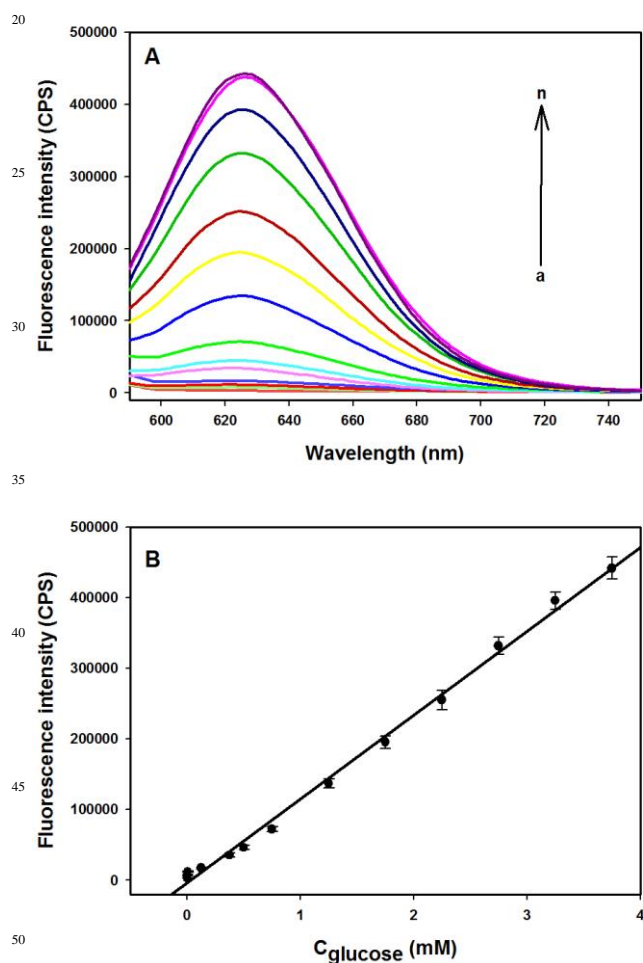


**Fig.4** (A) The fluorescence emission spectra of the sensing system with different concentrations of glucose (from a to n): 0  $\mu\text{M}$ , 0.75  $\mu\text{M}$ , 5  $\mu\text{M}$ , 125  $\mu\text{M}$ , 375  $\mu\text{M}$ , 0.5 mM, 0.75 mM, 1.25 mM, 1.75 mM, 2.25 mM, 2.75 mM, 3.25 mM, 3.75 mM, 4.5 mM. (B) The linear relationship between the fluorescence increase and the concentration of glucose. The concentration of DNA used here was all 1.0  $\mu\text{M}$ . Error bars represented standard deviations from three repeated experiments.

performance of the proposed sensing system. To examine the specificity of the DNA-Ag NCs probe towards glucose. Glycine, L-Cysteine, fructose, maltose, lysine, galactose and histidine were added into the sensing system instead of glucose to investigate the specificity. As shown in Fig. 5, the fluorescence intensity increased obviously after addition of glucose, but there were no significant differences between the blank after addition of the other interferents, indicating the high specificity of glucose. These results clearly indicated that the proposed method could serve as a high selectivity fluorescence probe for glucose detection.

As we all known, antioxidants, such as ascorbic acid (vitamin C), are the scavengers of free radicals. To prove that

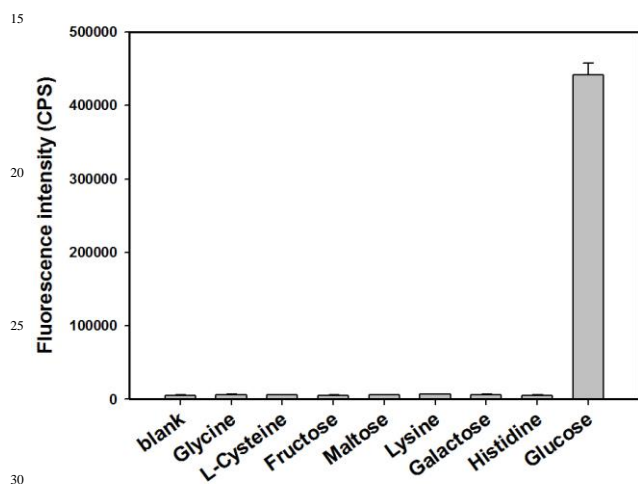


**Fig.5** Selectivity of the sensing system for glucose. The concentrations of glucose and histidine were 3.75 mM, The concentrations of all other interferents were fixed at 37.5 mM. Error bars represented standard deviations from three repeated experiments.

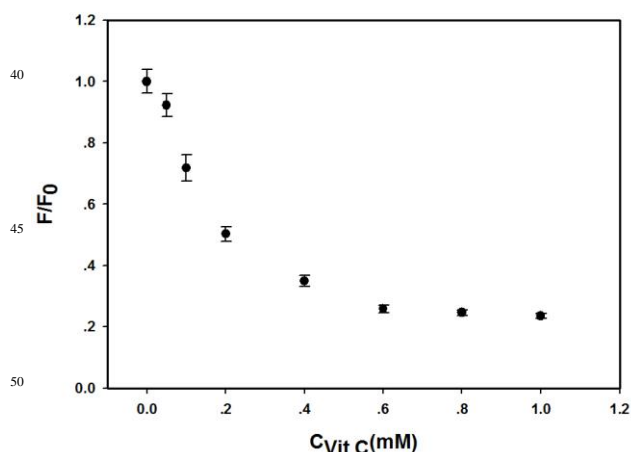


**Fig.6** Scavenging effect of ascorbic acid (vitamin C) on •OH. The concentration of glucose was 3.75 mM. Error bars represented standard deviations from three repeated experiments. F and F<sub>0</sub> are the fluorescence intensity of the sensing system in the presence and absence of ascorbic acid (vitamin C).

•OH was indeed produced in the sensing system, we added ascorbic acid (vitamin C) to the system. In the absence of Vit.C, •OH was not scavenged, so it did not have influence on the fluorescence of DNA-AgNC. However, in the presence of Vit.C, •OH was scavenged by Vit.C, B-DNA could not cleave into mono- or shortoligonucleotides fragment, so B-DNA hybridized with G-DNA. DNA-Ag NCs, which failed to hybridize with G-DNA, displayed very weak fluorescence. As shown in Fig. 6, F<sub>0</sub> is the fluorescence intensity of the sensing system in the absence of ascorbic acid (vitamin C), F is the fluorescence intensity of the sensing system in the presence of ascorbic acid (vitamin C). As F<sub>0</sub> did not change and F gradually decreased with the increasing of the ascorbic acid concentration, so F/F<sub>0</sub> gradually decreased with the increasing of the ascorbic acid concentration. This result is in keeping with the fact that ascorbic acid is the scavenger of •OH. Therefore, we have successfully proved that •OH is indeed produced in the sensing system.

In summary, a label-free and turn-on sensor for H<sub>2</sub>O<sub>2</sub> and glucose has been developed, it relies on the cleavage of ssDNA by •OH and the fluorescence enhancement effect when guanine-rich (G-rich) DNA sequences are in proximity to DNA-silver nanoclusters (DNA-Ag NCs). This sensing system has turned out to be reliable, sensitive, high S/N ratio, and high selective for H<sub>2</sub>O<sub>2</sub> and glucose detection. To evaluate the feasibility of the sensing system for glucose detection in biological samples, we have also successfully used this sensing system to detect glucose in urine. Furthermore, we also prove that •OH is indeed produced in the sensing system by adding antioxidants. Compared with some known assay methods, our DNA-Ag NCs based method demonstrates multifaceted advantages: first of all, the preparation of DNA-Ag NCs is facile, inexpensive and accessible to numerous labs, any special steps such as modification, separation, coating, and immobilization, are successfully avoided, which greatly decreases the operating difficulty. Second, this fluorescence probe is based on the fluorescence turn-on mode, which not only reduces the possibility of a false positive signal, but also enhances the detection sensitivity. Third, the concentration of H<sub>2</sub>O<sub>2</sub> or glucose could be monitored in real-time just by using a common spectrofluorometer. Therefore, our approach have turned out to be a successful paradigm in exploring the fascinating properties of DNA-Ag NCs, we expect that the novel strategy will open new opportunities for extending the applications of DNA-Ag NCs in multiple fields.

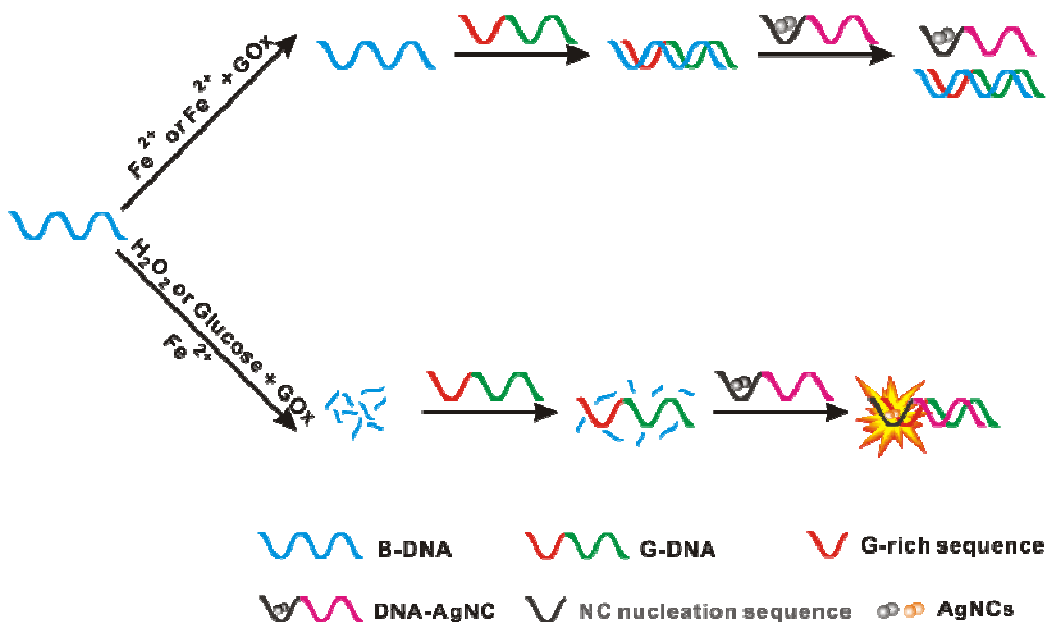
This work was supported by the National Natural Science Foundation of China (No. 21275045), NCET-11-0121, and Hunan Provincial Natural Science Foundation of China (Grant 12JJ1004).

## Notes and references

State Key Laboratory of Chemo/Bio-Sensing and Chemometrics, College of Chemistry and Chemical Engineering, Hunan University, Changsha, 410082, P. R. China. Tel.: +86-731-88821916; Fax: +86-731-88821916; E-mail addresses: xiachu@hnu.edu.cn.

Electronic Supplementary Information (ESI) available: [Experiment section, Supplementary Tables and Figures]. See

- DOI: 10.1039/b000000x/
- 1 L. Mao, P. G. Osborne, K. Yamamoto and T. Kato, *Anal. Chem.*, 2002, **74**, 3684–3689.
- 2 Y. Luo, H. Liu, Q. Rui and Y. Tian, *Anal. Chem.*, 2009, **81**, 3035–3041.
- 3 D. W. Gunz and M. R. Hoffmann, *Atmos. Environ. Part A. Gen. Top.*, 1990, **24**, 1601–1633.
- 4 N. V. Kiassen, D. Marchington and H. C. E. McGowan, *Anal. Chem.*, 1994, **66**, 2921–2925.
- 5 Y. Sang, L. Zhang, Y. F. Li, L. Q. Chen, J. L. Xu and C. Z. Huang, *Anal. Chim. Acta*, 2010, **659**, 224–228.
- 6 H. Jiang, Z. Chen, H. Cao and Y. Huang, *Analyst*, 2012, **137**, 5560–5564.
- 7 W. Jia, M. Guo, Z. Zheng, T. Yu, Y. Wang, E. G. Rodriguez and Y. Lei, *Electroanalysis*, 2008, **20**, 2153–2157.
- 8 J. E. Harrar, *Anal. Chem.*, 1963, **35**, 893–896.
- 9 A. H. Liang, S. M. Zhou and Z. L. Jiang, *Talanta*, 2006, **70**, 444–448.
- 10 L. Shang, H. Chen, L. Deng and S. Dong, *Biosens. Bioelectron.*, 2008, **23**, 1180–1184.
- 11 S. Oszwałdowski, R. Lipka and M. Jarosz, *Anal. Chim. Acta*, 2000, **421**, 35–43.
- 12 U. Pinkernell, S. Effkemann and U. Karst, *Anal. Chem.*, 1997, **69**, 3623–3627.
- 13 R. C. Matos, E. O. Coelho, C. F. d. Souza, F. A. Guedes and M. A. C. Matos, *Talanta*, 2006, **69**, 1208–1214.
- 14 J. Yuan and A. M. Shiller, *Anal. Chem.*, 1999, **71**, 1975–1980.
- 15 L. A. Terry, S. F. White and L. J. Tigwell, *J. Agric. Food Chem.*, 2005, **53**, 1309–1316.
- 16 N.G. Stan, D. Con and C. Trial, *Diabetes Care*, 2011, **34** (Suppl. 1), S4–S10.
- 17 D. M. Porterfield, *Biosens. Bioelectron.*, 2007, **22**, 1186–1196.
- 18 Y. Q. Lin, K. Liu, P. Yu, L. Xiang, X. C. Li and L. Q. Mao, *Anal. Chem.*, 2007, **79**, 9577–9583.
- 19 I. Al-Ogaidi, H. L. Gou, A. K. A. Al-kazaz, Z. P. Aguilar, A. K. Melconian, P. Zheng and N. Q. Wu, *Anal. Chim. Acta*, 2014, **811**, 76–80.
- 20 L. J. Xiao, Y. Q. Chai, H. J. Wang and R. Yuan, *Analyst*, 2014, **139**, 4044–4050.
- 21 M. A. Tabrizi and J. N. Varkani, *Sens. Actuator B*, 2014, **202**, 475–482.
- 22 S. Tierney, B. M. H. Falch, D. R. Hjelme and B. T. Stokke, *Anal Chem*, 2009, **81**, 3630–3636.
- 23 Y. Jiang, H. Zhao, Y. Q. Lin, N. N. Zhu, Y. R. Ma and L. Q. Mao, *Angew Chem*, 2010, **122**, 4910–4914.
- 24 J. C. Claussen, A. D. Franklin, A. Haque, D. M. Porterfield and T. S. Fisher, *ACS Nano*, 2009, **3**, 37–44.
- 25 W. B. Shi, Q. L. Wang, Y. J. Long, Z. L. Cheng, S. H. Chen, H. Z. Zheng and Y. M. Huang, *Chem Commun*, 2011, **47**, 6695–6697.
- 26 J. Solanki, O. P. Choudhary, P. Sen and J. T. Andrews, *Rev. Sci. Instrum.*, 2013, **84**, 073114.
- 27 G. G. Guilbault, P. J. Brignac and M. Zimmer, *Anal. Chem.*, 1968, **40**, 190.
- 28 H. Zhang, H. Huang, Z. H. Lin and X. G. Su, *Anal Bioanal Chem.*, 2014, **406**, 6925–6932.
- 29 X. L. Zhu, L. Y. Sun, Y. Y. Chen, Z. H. Ye, Z. M. Shen and G. X. Li, *Biosens. Bioelectron.*, 2013, **47**, 32–37.
- 30 Z. G. Mao, Z. H. Qing, T. P. Qing, F. Z. Xu, L. Wen, X. X. He, D. G. He, H. Shi and K. M. Wang, *Anal. Chem.*, 2015, **87**, 7454–7460.
- 31 Y. L. Wang, J. J. Chen and J. Irudayaraj, *ACS Nano*, 2011, **5**, 9718–9725.
- 32 F. Samari, B. Hemmateenejad, Z. Rezaei and M. Shamsipur, *Anal. Methods*, 2012, **4**, 4155–4160.
- 33 T. Vosch, Y. Antoku, J. C. Hsiang, C. I. Richards, J. I. Gonzalez and R. M. Dickson, *Proc. Natl. Acad. Sci. U.S.A.*, 2007, **104**, 12616–12621.
- 34 A. M. Derfus, W. C. W. Chan and S. N. Bhatia, *Nano Lett.*, 2004, **4**, 11–18.
- 35 S. F. Lee and M. A. Osborne, *J. Am. Chem. Soc.*, 2007, **129**, 8936–8937.
- 36 C. I. Richards, S. Choi, J. C. Hsiang, Y. Antoku, T. Vosch, A. Bongiorno, Y. L. Tzeng and R. M. Dickson, *J. Am. Chem. Soc.*, 2008, **130**, 5038–5039.
- 37 J. Sharma, H. C. Yeh, H. Yoo, J. H. Werner and J. S. Martinez, *Chem. Commun.*, 2010, **46**, 3280–3282.
- 38 J. T. Petty, J. Zheng, N. V. Hud and R. M. Dickson, *J. Am. Chem. Soc.*, 2004, **126**, 5207–5212.
- 39 E. J. Cho, J. W. Lee and A. D. Ellington, *Annu. Rev. Anal. Chem.*, 2009, **2**, 241–264.
- 40 H. C. Yeh, J. Sharma, J. J. Han, J. S. Martinez and J. H. Werner, *Nano Lett.*, 2010, **10**, 3106–3110.
- 41 J. Park, J. Lee, C. Ban and W. J. Kim, *Biosens. Bioelectron.*, 2013, **43**, 419–424.
- 42 H. Ma, W. Wei, Q. Lu, Z. X. Zhou, H. N. Li, L. Q. Zhang and S. Q. Liu, *Anal. Methods*, 2014, **6**, 6082–6087.
- 43 W. Wang, G. J. Lee, K. J. Jang, T. S. Cho and S. K. Kim, *Nucleic Acids Res.*, 2008, **36**, e85–e85.
- 44 L. H. Cao, J. Ye, L. L. Tong and B. Tang, *Chem. Eur. J.*, 2008, **14**, 9633–9640.
- 45 W. N. Liu, D. Ding, Z. L. Song, X. Bian, X. K. Nie, X. B. Zhang, Z. Chen and W. H. Tan, *Biosens. Bioelectron.*, 2014, **52**, 438–444.
- 46 A. L. Hu, Y. H. Liu, H. H. Deng, G. L. Hong, A. L. Liu, X. H. Lin, X. H. Xia and W. Chen, *Biosens. Bioelectron.*, 2014, **61**, 374–378.
- 47 S. A. Khan, G. T. Smith, F. Seo and A. K. Ellerbee, *Biosens. Bioelectron.*, 2015, **64**, 30–35.



A label-free and turn-on strategy for H<sub>2</sub>O<sub>2</sub> and glucose detection based on the cleavage of ssDNA by •OH and the fluorescence enhancement effect when guanine-rich (G-rich) DNA sequences are in proximity to DNA-silver nanoclusters (DNA-Ag NCs).